

Article

## Detection of Multidecadal Changes in UVB and Total Ozone Concentrations over the Continental US with NASA TOMS Data and USDA Ground-Based Measurements

Zhiqiang Gao <sup>1,2,\*</sup>, Wei Gao <sup>1</sup> and Ni-Bin Chang <sup>3</sup>

<sup>1</sup> USDA UV-B Monitoring and Research Program, Natural Resource Ecology Laboratory, Colorado State University, Fort Collins, CO 80525, USA; E-Mail: wgao419@gmail.com

<sup>2</sup> Institute of Geographical Sciences and Natural Resources Research, Chinese Academy of Sciences, Beijing 100101, China

<sup>3</sup> Department of Civil, Environmental and Construction Engineering, University of Central Florida, Orlando, FL 32816, USA; E-Mail: nibinchang@gmail.com

\* Author to whom correspondence should be addressed; E-Mail: gaoland@gmail.com; Tel.: +1-970-491-3609; Fax: +1-970-491-3600.

Received: 10 November 2009; in revised form: 17 December 2009 / Accepted: 30 December 2009 / Published: 5 January 2010

---

**Abstract:** Thinning of the atmospheric ozone layer leads to elevated levels of Ultraviolet-B (UVB) at the Earth's surface, resulting in an increase of health risks to living organisms due to DNA damage. This paper examines the multidecadal changes of total column ozone from 1979 to 2005 with the aid of ground-based UVB stations using the ultraviolet multifilter rotating shadow-band radiometer (UV-MFRSR). For the purpose of demonstration, four USDA ground stations, WA01, CO01, MD01, and AZ01, were selected for detailed comparisons against the satellite data. The major finding of this study is that over the course of the time series, on a monthly scale, the UV index (UVI) has increased at the four selected USDA stations while total ozone has decreased in the continental USA over the past three decades and spatial distributions of UVI and total ozone have shown substantial variations from coastal zones to the Midwest Regions of the USA, yet the tendency toward recovery of ozone layer in the continental USA cannot be fully confirmed. This leads to a conclusion that the UVI changes might have been influenced by other factors in addition to the total ozone in the atmospheric environment across at least 76% of the continental USA.

**Keywords:** UVB; total ozone; Nimbus-7/TOMS; spatial analysis

---

## 1. Introduction

Concern over the harmful effects of increased solar UV radiation on the biosphere due to thinning of the atmospheric ozone layer has prompted extensive efforts to characterize it at the Earth's surface, which can help identify its impacts over differing latitudes [1–3]. The spatial coverage of UV radiation monitoring sites is still too sparse and the historical record is still too short to determine the global-scale UV pattern and trends using UV radiation measurements alone [4,5]. Space-borne observation can provide information on two key parameters that determine UV irradiance: total ozone amount and the cloud transmittance or reflectivity. Satellite UV retrievals have been developed using the total ozone mapping spectrometer (TOMS) onboard the National Aeronautical and Space Administration (NASA) Nimbus 7 satellite to provide continuous spatial coverage over the whole planet. However, the ground-based network is better suited to monitoring local conditions than the currently large-pixel (100 km) satellite estimates. Consequently, TOMS, which has provided both total ozone and cloud reflectivity measurements since 1979, is an important source of derived UV data [6–8].

Approaches using TOMS data should be deemed as critical alternatives to ground-based measurements for assessments of long-term total ozone. As a prelude to a full-scale causal investigation, an advanced intercomparison between total ozone and Ultraviolet-B (UVB) at differing spatial and temporal scales across the continental USA is of value to explore any abnormal trends and unusual correlations [9–11]. However, TOMS data had anomalies in the year 2000 and Earth Probe TOMS began to experience two problems after 2000, including a drop in throughput of the instrument of about 50%, and a cross track bias such that ozone measured when looking to the far left of the orbit track is 2% to 3% lower than ozone measured when looking to the far right of the orbit track. Using the TOMS total ozone data solely after 2000 might result in misleading trend implications, and this compounds the research challenges.

To gain a more accurate estimate of total ozone, research focus has been placed upon the improvement of data assimilation algorithms for both satellite data and ground-based measurements. McCormack and Hood [12] used a form of the linearized steady state ozone continuity equation to model the spatial distribution of total ozone in the Northern Hemisphere (NH) winter for the period 1979–1991. A significant decrease of the wave-induced variance in the wintertime total ozone distribution was indicated over the 1979–1991 period, which is consistent with the observed longitude dependence of total ozone trends in NH winter. Ground-based measurements permit relatively precise local studies on UV irradiance and its relationship with atmospheric components. Long-term decreases in summertime ozone over Lauder, New Zealand (45°S), are shown to have led to substantial increases in peak UV radiation intensities [13]. The increasing trend of UV irradiance has been confirmed by several projects in recent years. Gao *et al.* [7] developed a methodology for direct-Sun ozone retrieval using the ultraviolet multifilter rotating shadow-band radiometer (UV-MFRSR). This approach allows for the real-time measurement of total vertical column ozone at ground-based stations; three such

stations were tracked in this study. This capability fosters advanced intercomparisons between the daily UV erythemal doses and total column ozone calculated with any space-borne data and observed at the United States Department of Agriculture (USDA) ground-based network, as was pursued in the study reported here.

Because the downward trends in ozone had already been occurring for several years before the UV radiation measurements became available, it would be of interest to compare the total ozone concentrations between USDA ground-based measurements and NASA TOMS satellite data at differing temporal and spatial scales across the continental USA [14–18]. To address such impacts, this paper presents a comparative analysis to examine the changes and inconsistencies of total ozone in recent years, investigating the temporal and spatial differences of both sources of data over the continental USA. Intercomparisons were made between the total column ozone calculated with the NASA Nimbus-7/TOMS UV algorithm and the total ozone concentrations from USDA ground-based network between 1979 and 2005. Four of the USDA ground stations, specifically WA01 (Pullman, Washington, 46.76°N, 117.192°W), CO01 (Nunn, Colorado, 40.806°N, 104.756°W), MD01 (Queenstown, Maryland, 38.917°N, 76.151°W), and AZ01 (Flagstaff, Arizona, 36.059°N, 112.184°W), were selected for detailed investigations of the temporal changes of and the correlations between the UV index (UVI) [19] and total ozone. This is followed by spatial analyses of multi-year UVI and total ozone data computed from TOMS and UV-MFRSR over the continental USA. Such an in-depth spatial and temporal assessment of both UVB and total ozone is of significance for future sustainable development by human societies.

## 2. Materials and Methods

### 2.1. USDA UVB Data

The USDA UV-B Monitoring and Research Program (UVMRP) is a program of the USA Department of Agriculture's Cooperative State Research, Education and Extension Service (CSREES). The UV-B Radiation Monitoring and Research Programs began in 1995, and 37 sites now exist across the United States. All data from the network is captured by on-site data loggers and downloaded over phone each evening. Data is made available to the scientific community, as well as the general public, for next day retrieval via the network's World Wide Web site (<http://uvb.nrel.colostate.edu>). These stations use the UV-MFRSR sensor, which is a seven-channel UV version of the visible multifilter rotating shadow-band radiometer, to measure total horizontal and diffuse horizontal irradiances. The seven channels are created by ion-assisted-deposition filters with a nominal bandwidth of 2 nm at full width half maximum (FWHM) and nominal band centers at 300, 305, 311, 317, 325, 332 and 368 nm. There is filter-to-filter variation in the nominal wavelength center ( $\pm 0.5$  nm). The direct beam is obtained by subtraction of the diffuse horizontal from the total horizontal irradiance and includes the corrections made, such as Langley calibration (<http://uvb.nrel.solostate.edu/UVB/LangleyCalibrationDataprocessing.jsf>). The measurement is completed in less than 5 s at all wavelengths. All three components are recorded every 20 s and averaged to 3 min intervals.

The UV-MFRSR measures the relative intensities of selected pairs of UV wavelengths, as with the Dobson spectrophotometers, in order to estimate direct-Sun total column ozone. The first pair used in

this study consists of 305 nm and 325 nm wavelengths. Light from both wavelengths is attenuated owing to scattering by air molecules and dust particles in passing through the atmosphere to the instrument. Dobson [21] developed mathematical equations to calculate total column ozone from direct observation of the Sun [also summarized by Komhyr [20]. The total column ozone ( $\Omega$ ), expressed in Dobson Units (1 DU =  $10^{-3}$  cm pure ozone at standard temperature and pressure), as estimated from a single wavelength pair  $\lambda$  and  $\lambda'$  is [7,20,21]:

$$\Omega = \frac{N(\beta_{\lambda} - \beta_{\lambda'})m(P/P_0) - (\delta_{\lambda} - \delta_{\lambda'})\sec Z}{(\lambda_{\lambda} - \lambda_{\lambda'})\mu} 10^3 \quad (1)$$

where:

$$N = \ln \frac{V_{o\lambda}}{V_{o\lambda'}} - \ln \frac{V_{\lambda}}{V_{\lambda'}} \quad (2)$$

In Equations (1) and (2),  $V_{\lambda}$  is the measured voltage at the ground at wavelength  $\lambda$ , in millivolts,  $V_{o\lambda}$  is the extraterrestrial voltage intercept at zero air mass at wavelength  $\lambda$ , in millivolts;  $V_{\lambda'}$  is the measured voltage at the ground at wavelength  $\lambda'$ , in millivolts;  $V_{o\lambda'}$  is the extraterrestrial voltage intercept at zero air mass at wavelength  $\lambda'$ , in millivolts.  $\beta_{\lambda}$  is the Rayleigh scattering coefficient (molecular optical depth) at wavelength  $\lambda$ , unitless  $m$  is the air mass corresponding to solar zenith at the time of the direct normal irradiance measurement, in g;  $P$  is the observed station pressure, in millibars;  $P_0$  is the mean sea level pressure, in millibars;  $\delta_{\lambda}$  is the scattering coefficient (optical depth) of aerosol particles at wavelength  $\lambda$ , unitless; and  $Z$  is the Solar zenith angles, in degrees.

With this methodology, total vertical column ozone between 1998 and 2005 was retrieved from 37 stations over the continental USA. The broadband UVB-1 Pyranometer that is employed, manufactured by Yankee Environmental Systems, measures global irradiance in the UVB spectral range of 280–320 nm. Figure 1 shows the locations of all 37 ground-based stations and highlights the four sites (circled sites) selected for a detailed statistical analysis, namely stations WA01, MD01, CO01, and AZ01. These four stations are well distributed geographically, with WA01 located in the north, AZ01 the south, CO01 the center, and MD01 the east of the United States.

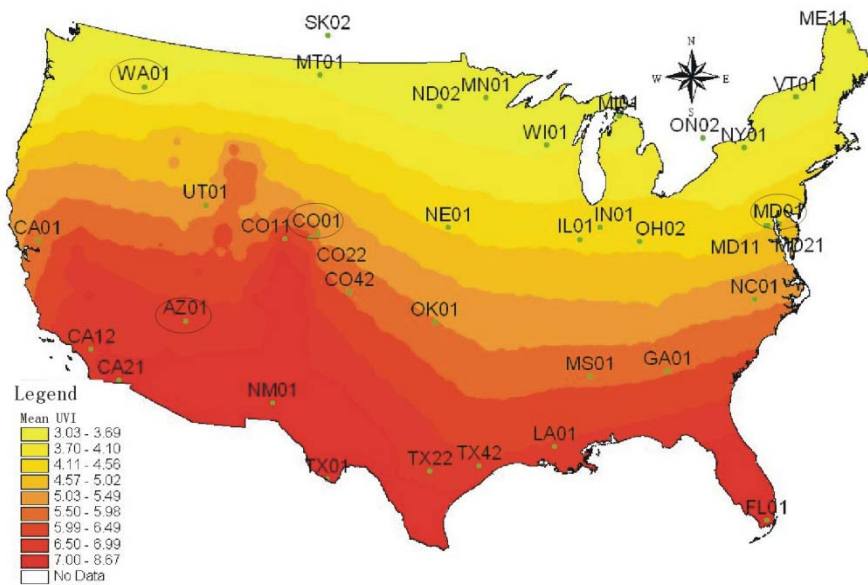
## 2.2. TOMS Data

In contrast to ground observations, satellites provide complete global coverage at a moderate resolution with standardized sensors. UV has been observed from space for more than 30 years. Early satellite UV measurements were made by the Backscatter Ultraviolet (BUV) sensor onboard the Nimbus 4, which was launched in 1970 and continued functioning for several years. Nimbus 7 provided the longest high-quality UV space-borne observation from 1978 to 1993 with TOMS. This dataset can be used for monitoring long-term trends in total column ozone. Further, it is useful for investigating seasonal chemical depletions in ozone occurring in both the southern and northern hemisphere polar springs.

The total column ozone retrieval from satellite data uses a normalized radiance, which is defined as the ratio of the backscattered Earth radiance to the incident solar irradiance. Calculating this ratio requires periodic measurements of the solar irradiance. To measure the incident solar irradiance, the

TOMS scanner is positioned to view an aluminum diffuser plate that reflects sunlight into the instrument. Retrieval of total column ozone is based on a comparison between the measured normalized radiances and radiances derived by radiative transfer calculations for different ozone amounts and the conditions of the measurement [22].

**Figure 1.** Map of the 37 USDA ground stations. Statistical analyses focused on the four circled stations.



The Erythemal Exposure data product of TOMS is an estimate of the daily integrated ultraviolet irradiance, calculated using a model of the susceptibility of caucasian skin to sunburn (erythema). This can be interpreted as an index of the potential for biological damage due to solar irradiation, given the column ozone amount and cloud conditions on each day. The Erythemal Exposure (Exp) is defined by the integral [22]:

$$\text{Exp} = \frac{1}{d_{\text{es}}} \int_{280\text{nm}}^{400\text{nm}} d_{\lambda} S(\lambda) W(\lambda) \int_{t_{\text{ss}}}^{t_{\text{sr}}} d_t C(\lambda, \vartheta, \tau_{\text{cl}}) F(\lambda, \vartheta, \Omega) \quad (3)$$

where  $d_{\text{es}}$  is the Earth-sun distance, in A.U.;  $S$  is the solar irradiance incident on the top of the atmosphere at 1 A.U. ( $\text{nW m}^{-2} \text{nm}^{-1}$ );  $W$  is the biological action spectrum for erythemal damage, in B.D.  $\text{m}^{-2}$ , where B.D. = Biological Damage;  $t_{\text{sr}}$  and  $t_{\text{ss}}$  are the time of sunrise and sunset, in radians;  $C$  (unitless) is the cloud attenuation factor;  $\tau_{\text{cl}}$  is the cloud optical thickness, in mbar;  $\vartheta$  is the solar zenith angle (function of time,  $t$ ), in radians; and  $F$  (unitless) is the spectral irradiance at the surface under clear skies, normalized to unit solar spectral irradiance at the top of the atmosphere.

### 2.3. UV-Index (UVI)

For UV induced erythema (sunburn), the action spectrum adopted by most international organizations is the CIE (Commission Internationale de l'Éclairage, International Commission on Illumination) action spectrum (E), using the method described by McKinlay and Diffey [23]. The

UV-Index (UVI) itself is an irradiance scale computed by multiplying the CIE irradiance in watts  $m^{-2}$  by 40. The clear sky value at sea level in the tropics is normally in the range 10–12 (250–300  $mWm^{-2}$ ) and 10 is an exceptionally high value for northern mid-latitudes. This scale has been adopted by the World Meteorological Organization (WMO) [19] and World Health Organization (WHO) and is in use in a number of countries. UV intensity is also described in terms of ranges running from low (0–2) to medium (3–5), high (6–7), very high (8–10) and extreme values (11+).

### 3. Results and Discussion

#### 3.1. Statistical Analysis of UVI and Total Ozone Data

For the four representative ground-based stations, we produced the derived daily UVI data measured by the broadband UVB-1 Pyranometer and the TOMS instrument from 1999 to 2005 for statistical analyses (Table 1). Similar analysis was also performed for total ozone data measured by UV-MFRSR and TOMS within the comparable time period (Table 2). Both Tables 1 and 2 summarize the mean, median, minimum, maximum, standard error, standard deviation, and correlation coefficients between these two datasets for UVI and total ozone, revealing how they each vary relative to the mean and their correlations with each other.

**Table 1.** Monthly statistical analysis of UVI data collected by four ground-based USDA stations and the TOMS Data (1999–2005, unitless).

	WA01		CO01		MD01		AZ01	
	USDA	TOMS	USDA	TOMS	USDA	TOMS	USDA	TOMS
<b>Minimum</b>	0.48	0.25	0.98	1.32	1.25	1.18	2.20	2.19
<b>Maximum</b>	8.86	9.22	9.82	10.97	7.6	8.19	12.14	11.36
<b>Mean</b>	3.80	4.00	5.20	5.80	4.24	4.71	6.76	6.94
<b>Median</b>	3.42	3.98	5.20	6.18	3.81	4.95	7.13	7.60
<b>Std. Error</b>	0.30	0.33	0.35	0.38	0.25	0.29	0.38	0.38
<b>Correlation Coefficient</b>	0.99		0.98		0.98		0.98	

Table 1 shows that the absolute disparity between ground-based stations and TOMS derived UVI data ranged from 0.2 to 0.6 units, and the relative disparity between the two sources ranged from 5% to 12%. The minimum and maximum of UVI from these two sources were close and their absolute disparity ranged from 0.1 to 0.2, respectively. Correlation coefficients between the two sources were over 98%, indicating that they are temporally highly correlated. On the other hand, Table 2 shows that total ozone measured by the ground-based stations was always larger than those derived from the TOMS data in terms of mean, maximum and median. The absolute disparity between mean total ozone based on these two sources ranged from 0 to 9 DU, and the relative disparity varied from 0% to 20.7%. Correlation coefficients between these two sources were over 90%; therefore they are highly correlated temporally also.

These summary statistics reveal the degree of correspondence between the two data sources. It may be concluded that the mean, median, minimum and maximum of the multi-year time series are very close for both UVI and total ozone between these two sources. Both standard errors and standard deviations were very similar across the four stations, indicating that similar fluctuations due to planetary- and medium-scale waves occurred at these sites during the study period. Such findings support advanced spatial analyses.

**Table 2.** Monthly statistical analysis of total ozone data collected by four ground-based USDA stations and the TOMS Data (1999–2005, unit: DU)

	WA01		CO01		MD01		AZ01	
	USDA	TOMS	USDA	TOMS	USDA	TOMS	USDA	TOMS
<b>Minimum</b>	248	261	258	251	263	254	249	244
<b>Maximum</b>	402	378	365	365	378	362	340	350
<b>Mean</b>	328	319	307	302	317	310	294	294
<b>Median</b>	330	317	303	298	317	312	292	292
<b>Std. Error</b>	3.40	3.20	2.52	2.59	2.58	2.68	2.13	2.38
<b>Correlation Coefficient</b>	0.92		0.94		0.90		0.96	

### 3.2. The Station Changes Analysis of UVI and Total Ozone Using TOMS Data

Yearly averages of these observations from 1979 to 2005 may reveal a consistent trend between stations, thereby supporting the multi-year spatial analyses. Figures 2, which plot the time-series of UVI and total ozone associated with each data source for the CO01 station, confirm the consistency of the seasonal trend on one hand and identify possible interactions between UVI and total ozone variations on the other hand. To facilitate interpretation, separate subplots are presented for each of the four seasons at this CO01 station. Comparing such sequences associated with both data sources may enable us to identify the general trends and can also characterize how the patterns they detect differ geographically.

In Figure 2(a), the trend analysis for spring indicates that the UVI measurements showed an increasing long-term trend while the total ozone data showed a decreasing long-term trend from 1979 to 2005. Overall, the UVI measurements reached their minimum in 1996 followed by moderate fluctuations of UVI from 1997 to 2005. Station CO01 is located at elevations as 1641m, where contrasting trends of UVI and total ozone are very distinct. The negative correlation between the springtime UVI and total ozone were as very strong at this site: 0.89, indicating the impact of UV increase and OZONE reduction due to the plateau elevation.

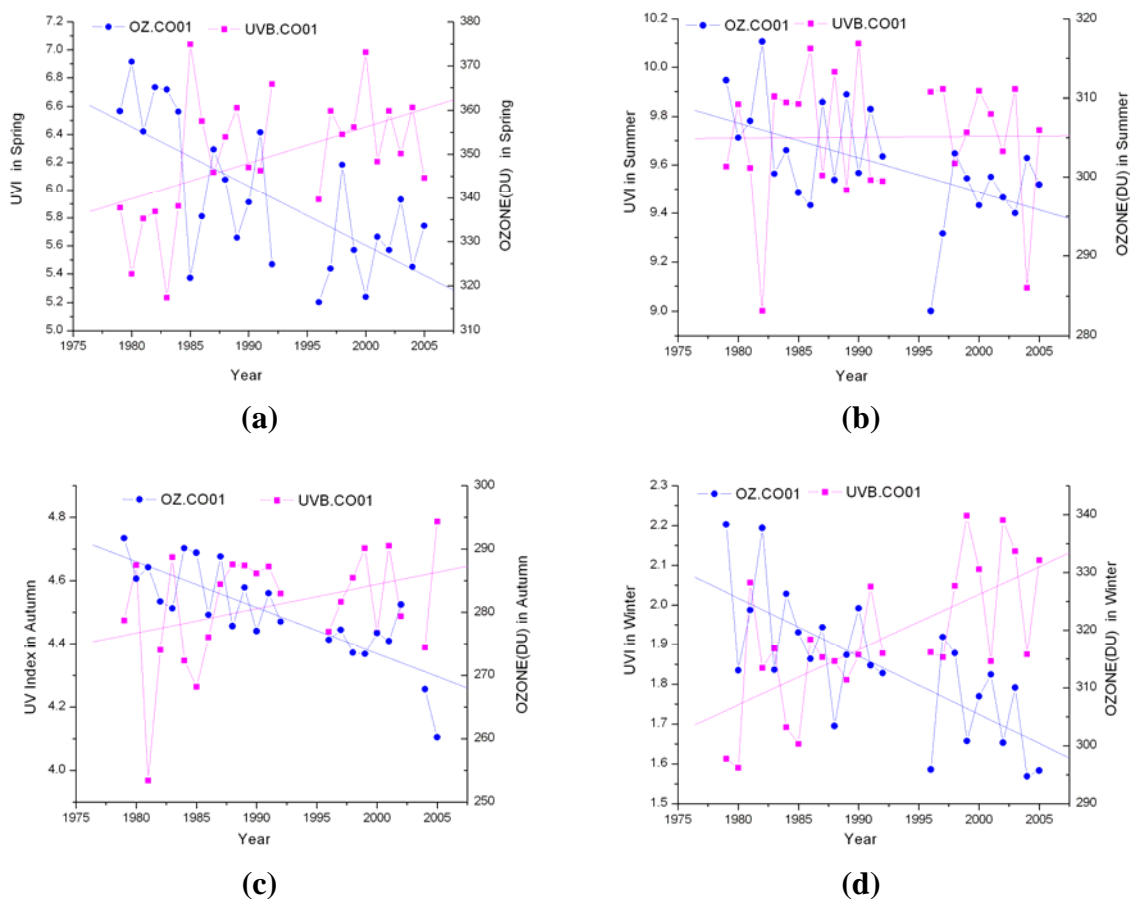
By the same token, Figure 2(b) exhibits a long-term trend analysis of UVI measurements and total ozone data in CO01 stations in summer. Over the 26-year time span, a generally decreasing trend of total ozone was also observed in summer. At the CO01 station, UVI measurements were slightly increasing over the 26 years of the study period; they revealed an apparent increasing trend from 1979 to 1992 and became stable and slightly decreasing during the rest of study period, having a valley

value in 2004. At the same time, total ozone was consistently decreasing. The negative correlation coefficient between the UVI measurements and total ozone data at CO01 was 0.64.

Figure 2(c) exhibits a long-term trend analysis of the UVI measurements and total ozone data over the CO01 stations in fall. The CO01 station revealed an increasing trend in UVI and a decreasing trend of the total ozone. The increasing trend of UVI measurements was accompanied by a decreasing trend of total ozone during the 26 years of the study period. In summary, the CO01 station collectively exhibited inconsistent fluctuations between the UVI measurements and total ozone data in the fall, ending up relatively low negative correlation coefficients over the 26 years of the study period. These negative correlations were 0.21 at the CO01 station.

Figure 2(d) exhibits a long-term trend analysis of UVI measurements and total ozone data at CO01 stations in winter. In general, an increasing trend of UVI measurements occurred with a decreasing trend of total ozone at all four stations over the 26 years of the study period. The CO01 station exhibited a homogeneous increasing trend of UVI measurements and a homogeneous decreasing trend of total ozone data in the study period. The relatively better consistency of the conflicting trends between the UVI measurements and the total ozone data resulted in larger negative correlation coefficients. Consequently, they are 0.50 at the CO01 station.

**Figure 2.** Seasonal trend analysis of the UVI and total ozone deviations relative to the yearly means with TOMS data. (a) CO01 multi-year seasonal variations in Spring; (b) CO01 multi-year seasonal variations in Summer; (c) CO01 multi-year seasonal variations in Autumn; (d) CO01 multi-year seasonal variations in Winter.





In summary, the UVI measurements were generally increasing and the total ozone data were mainly decreasing from 1979 to 2005, supporting the well established expectation that UV radiation reaching Earth's surface has increased with a concomitant decline in the ozone layer. Site specific discrepancies did exist, however, leading to room for further investigation. The increasing trend of UVI measurements and the decreasing trend of total ozone were strongest at the CO01 station, which is located on plateau elevation at middle latitude. The negative correlation coefficients between the UVI measurements and total ozone data were relatively high in spring and summer, but low in fall and winter.

### 3.3. Spatial Analysis of UVI and Total Ozone Using TOMS Data

Influences of ground reflectivity and topography on erythemal exposure are keen. Using Earth Probe/TOMS (EP/TOMS) data may enable us to analyze and present the multi-year pixel-based mean and standard deviation of both UVI and total ozone across the continental USA. Based on the yearly data from 1979 to 2005, excluding 1993, 1994 and 2003 due to the missing of TOMS data, scientific investigation of incremental differences in mean UVI between the periods of 2000–2005, 1990–2000, and 1980–1990 may help understand spatial variation of UVI over differing time periods. These efforts address the following scientific questions: (1) How does UV climate vary over different geographical regions? (2) To what extent are the changes of total ozone related to the changes of UVI across differing regions? (3) What type of insight can we gain from the integrated temporal and spatial evidence of UVI and total ozone variations? And (4), can we improve the forecasting capability of UVI based on such an integrated temporal and spatial analysis?

Figure 3 summarizes the multi-year mean and standard deviation of both UVI and total ozone across the continental USA from 1979 to 2005. As evidenced by Figure 3a,b driven by the same TOMS data, the multi-year mean distributions of total ozone and UVI across the continental USA exhibit consistent spatial patterns that implies the higher the total ozone, the lower the UVI is. Yet this is not the case along the USA-Canada borders. The UVI multi-year mean gradually decreases northward and the contour lines are approximately parallel with the latitudes. Both present a convex shape to the north along the Rocky Mountains because of the influence of high elevation in Arizona, New Mexico, and the Colorado Plateau, where the maximum UVI multi-year mean of 8.67 occurred.

The minimum value of the UVI multi-year mean was 3.03, which occurred at the northern border of the United States. On the other hand, the magnitude of total ozone gradually decreases southward. The contour lines are also approximately parallel with the latitudes, but are convex to the north along the Rocky Mountains, as with UVI. The minimum occurred over the Colorado Plateau, which is where the maximum UVI occurred.

Figures 3c,d are multi-year standard deviation distribution maps of total ozone and UVI across the continental USA. The standard deviation is a measure of the variability or dispersion of a statistical data set. A low standard deviation indicates that the data points tend to be very close to the mean, whereas high standard deviation indicates that the data are spread out over a large range of values. So in Figure 3, the higher the standard deviation, the higher the annual fluctuation. Figure 3c shows that areas of higher annual fluctuations of total ozone were the Columbia Plateau and the Great Lakes, and lower annual fluctuations of total ozone occurred around the USA states bordering the Gulf of Mexico.

and the Great Plateau. Figure 3(d) shows that UVI had higher annual fluctuations at the southern Rocky Mountains, Colorado Plateau, northern Great Basin and western Columbia Basin.

**Figure 3.** Multi-year mean and standard deviation of UVI and total ozone across the continental USA from 1979 to 2005. (a) Multi-year mean of total ozone; (b) Multi-year mean of UVI; (c) Multi-year standard deviation of total ozone; (d) Multi-year standard deviation of UVI.

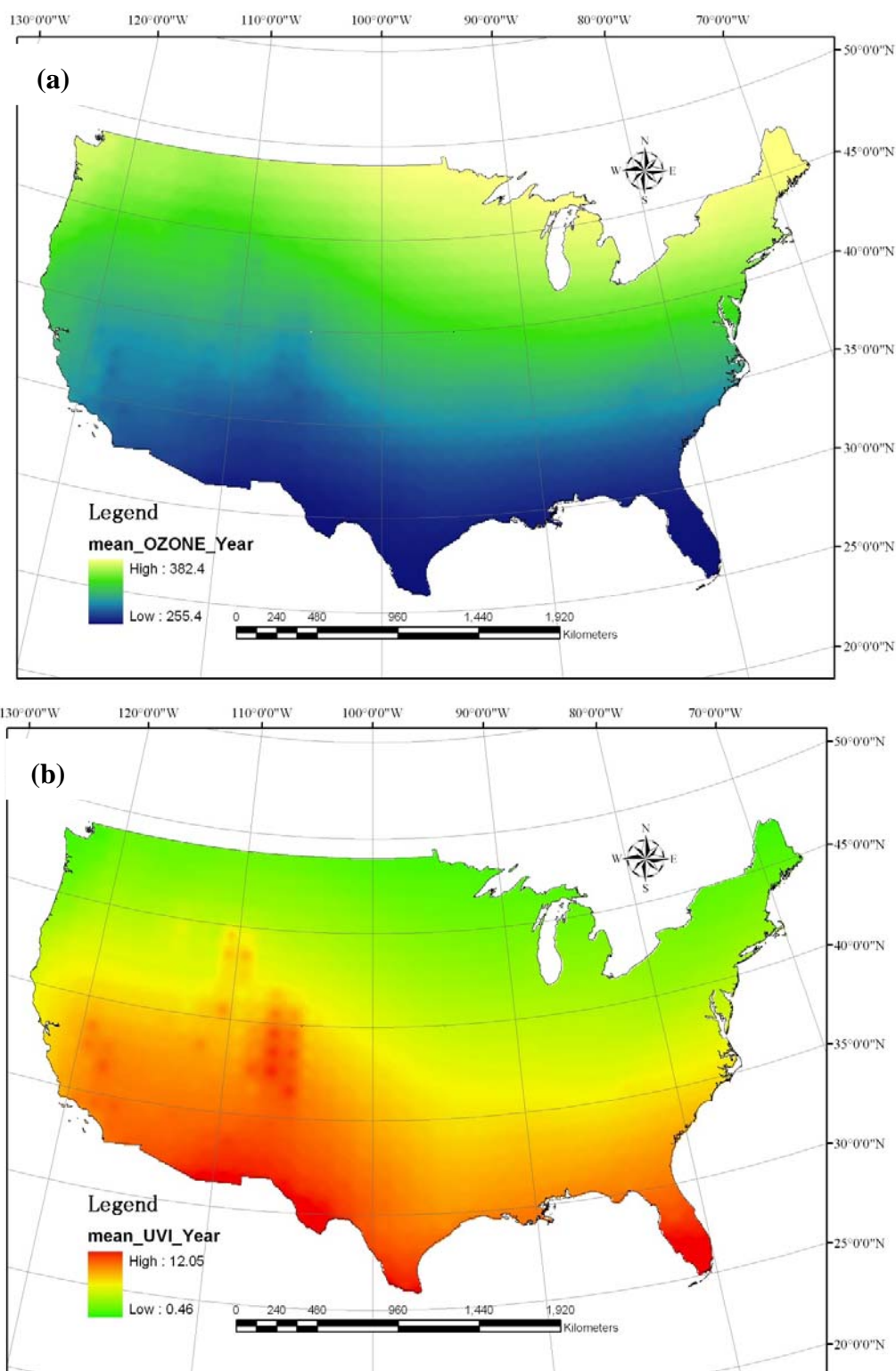
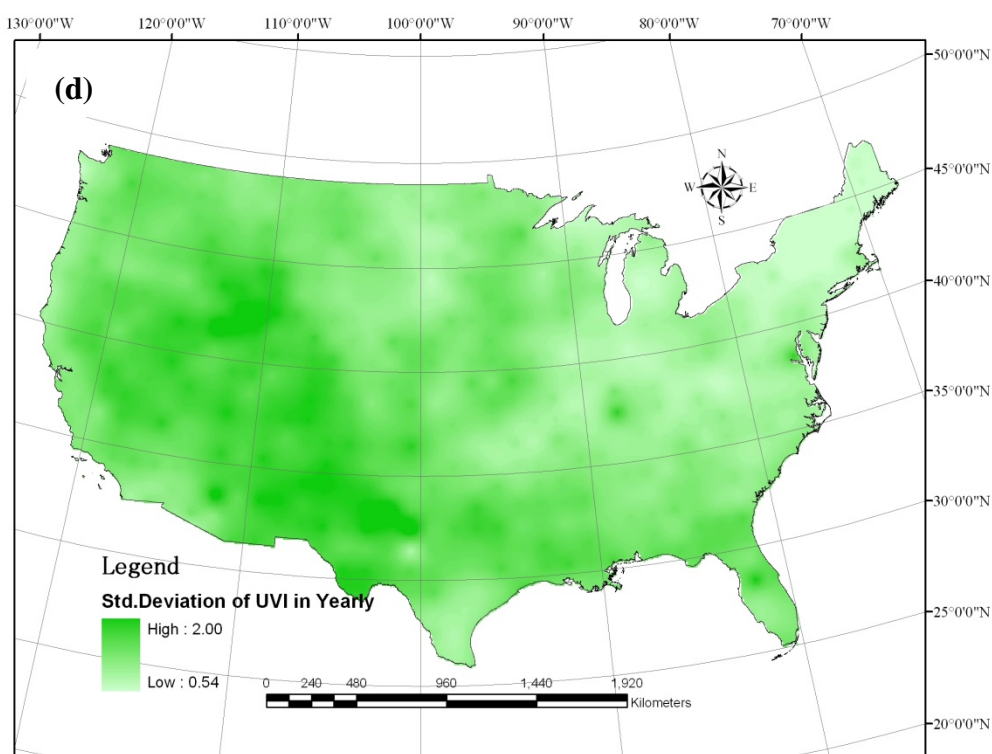
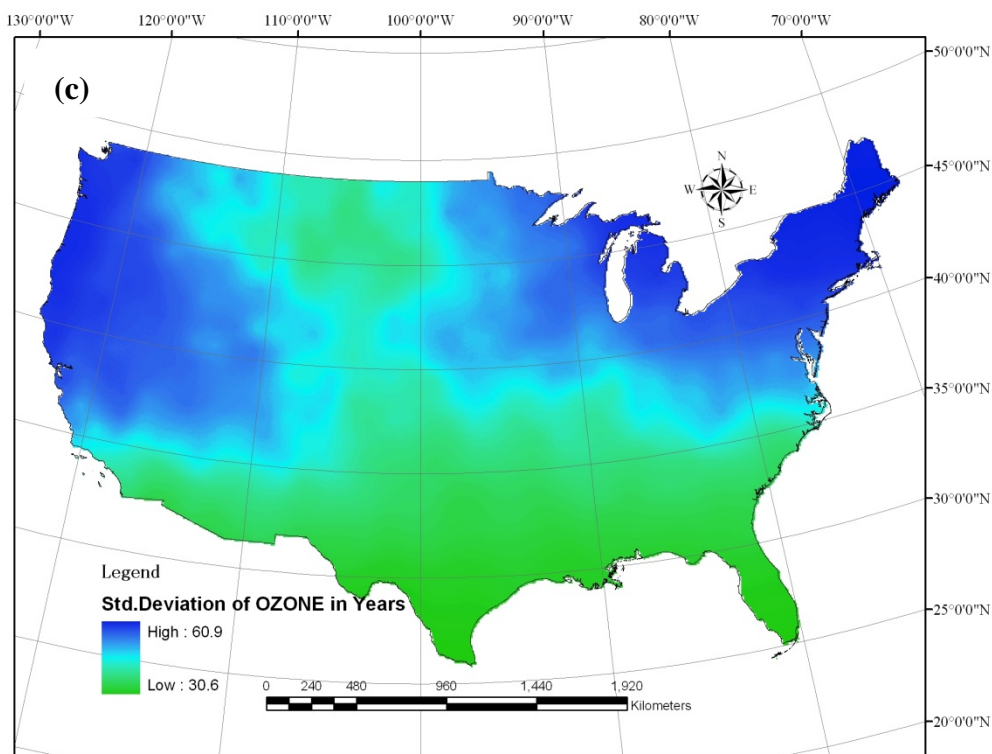


Figure 3. Cont.



In contrast, areas of lower annual fluctuations of UVI were the Great Lakes, Central Plains, Great Plains, and Columbia Basin. As a whole, the annual fluctuations of total ozone were relatively high in northern states and had no specific linkage with the elevation; yet the annual fluctuations of UVI had an obvious association with the elevation. This implies that the annual fluctuations of UVI are high at relatively higher altitudes.

Figure 4a is a map of the difference in UVI between the periods of 1980–1989 and 1990–1999. It shows that 99.5% of the continental USA had either a positive or zero change in UVI, implying that the UVI of the 1990s is generally higher than that of the 1980s. Increases were greatest along the Rocky Mountains, Colorado Plateau, Great Basin, New Mexico, Texas, Appalachian Mountains, and the middle-northern area of the Coastal Plain.

**Figure 4.** Multi-year spatial variation of UVI changes in the continental USA. (a) UVI difference between 1980s and 1990s; (b) UVI difference between 1990s and 2000s.

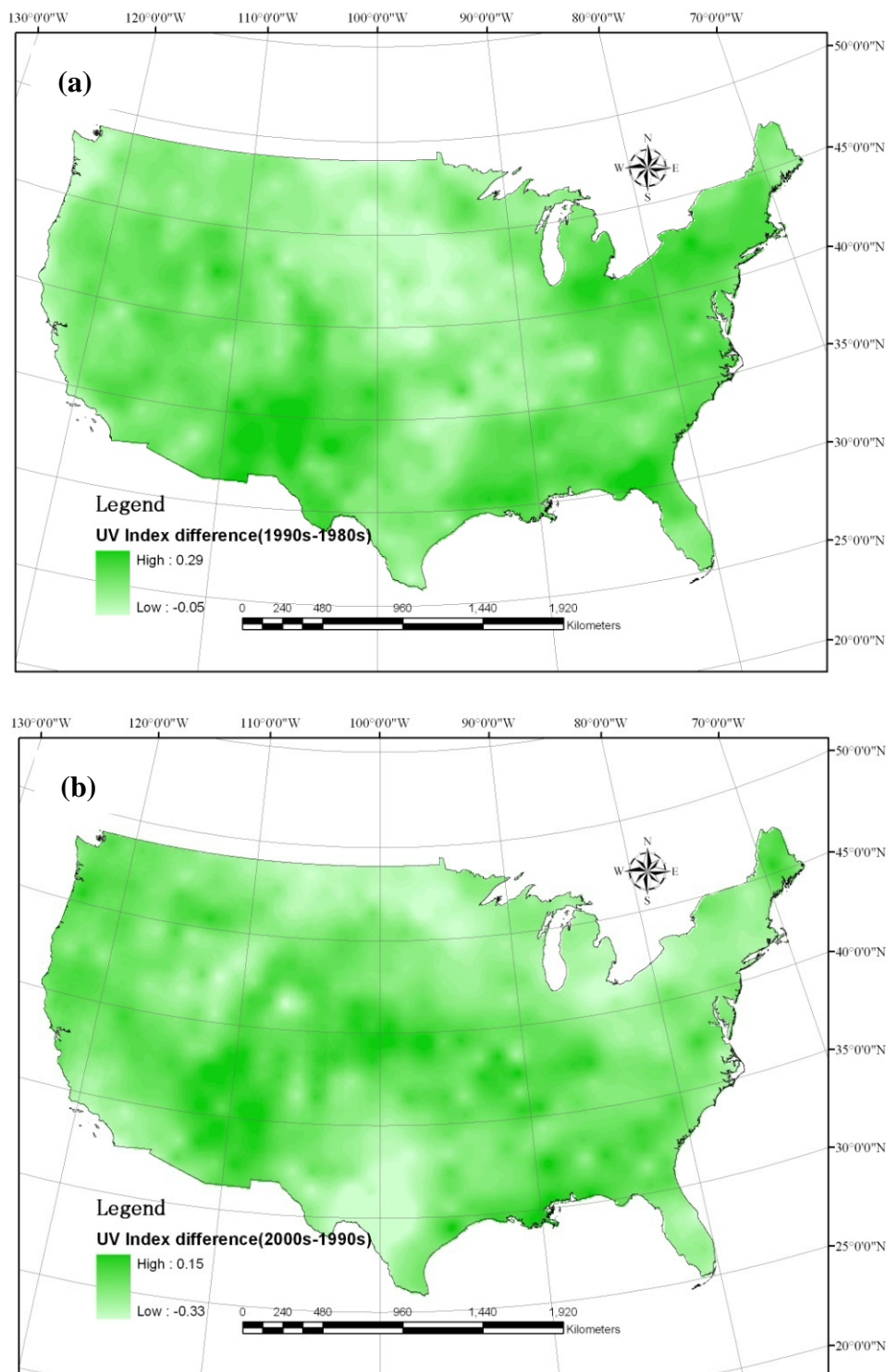


Figure 4(b) is a UVI difference distribution map between the period of 1990–1999 and 2000–2005. Between these time periods, 76% of the continental USA had negative difference, implying that UVI of the 1990s is generally higher than that of the 2000s. What explains this recent decrease of UVI? This question may trigger research of other factors affecting UVI. For instance, if aerosol and cloud data are available for the comparable time period, this investigation may be extended, leading to an exploration of the environmental processes associated with cyclical changes of UVI. This is related to global dimming, in which atmospheric aerosols and other particulates have been linked to reductions in shortwave radiation.

### 3.4. Final Remarks

Many literatures have found that the total column ozone in the Northern Hemisphere (NH) middle latitudes has started recovery or at least has not decreased since 1997, based on data derived from models, ground-based measurements and remote sensing. Previous work [24,25] and recent analysis [26] support three signatures as a basis for investigating ozone recovery. These signatures correspond to the latitudinal, seasonal and altitudinal dependences of observed changes. Recent data suggest that total column ozone abundances have at least not decreased over the past eight years (1997–2005) for most of the world including the NH middle latitude [27]. Reinsel *et al.* [28] analyzed total ozone data from satellite and ground-based measurements including the merged TOMS and Solar Backscatter UltraViolet (SBUV) merged ozone data (MOD) used here over the period 1978–2002 and identified a positive, significant change in trend after 1996 in the NH middle latitudes, even after accounting for some dynamical variables in their statistical model. Andersen *et al.* [26] found that there is substantial interest in examining the emerging data, particularly since 1996, for signs of recovery. However, most models suggest a more gradual recovery with an increasing magnitude of recovery rates over time. Previous studies including Reinsel [29] and Newchurch *et al.* [30] have examined changes in the ozone profile as well as total column ozone. Hadjinicolaou [31] found the positive ozone trend for the 1994–2003 study period in their dynamically-driven model ozone that explains all the observed trend, suggests that the notion of an early sign of a turnaround due to chemical recovery in total ozone should be treated with caution. Their results are qualitatively consistent with the chemistry climate modeling (CCM) results of Schnadt and Dameris [32] that predict an accelerated NH ozone recovery from 1990 to 2015 due to tropospheric dynamical changes (in contrast with some other CCMs). With this said above, since the continental USA is located in NH middle latitudes, potential errors in the USDA and TOMS methods for estimating ozone column amount from the UV measurements may arise from synergistic effects of atmospheric aerosols, cloud distribution, and other particulates.

In summary, the spatial analysis identified an increasing UVI in the following areas: the southern Rocky Mountains, Colorado Plateau, middle-Great Plains, southern Central Plains, and Coastal Plain; whereas the areas with a decreasing UVI were located in the northern and southern Great Plains, northern Central Plains, and the Great Lakes. The final spatiotemporal analysis found that the UVI was apparently increasing from 1979 to 1999 and decreasing during the period of 2000–2005 in most of the continental USA. This leads to a conclusion that the UVI changes might have been influenced by other factors in addition to the total ozone in the atmospheric environment across at least 76% of the continental USA in recent years.

#### 4. Conclusions

This paper compares UVI and total ozone obtained from USDA ground-based measurements and EP/TOMS data. For the four sites selected for demonstration, basic statistical analyses using the mean, standard deviation, correlation coefficients, and differences were performed to compare the multi-year UVI and total ozone variations. The findings confirm consistency between ground-based measurements and TOMS data. Total ozone measured at the CO01 station decreased over 1979 to 2005, yet the UVI was apparently increasing from 1979 to 1992, remained stable for a time, and then slightly decreased from 1995 to 2005. The negative correlation coefficients between the UVI measurements and total ozone data were relatively high in spring and summer, but they were low in fall and winter.

The UVI multi-year mean gradually decreases northward and the contour lines were approximately parallel with the latitudes, but presenting a convex shape to the north because of the elevation influence. The magnitude of total ozone gradually decreases southward and the contour lines are also approximately parallel with the latitudes, having a northward convex shape along the Rocky Mountains. The annual fluctuations of total ozone were relatively high in northern states and had no specific linkage with the elevation; yet the annual fluctuations of UVI had an obvious association with the elevation. This implies that the annual fluctuations of UVI are high at relatively higher altitudes. Annual UVI and total ozone were negatively correlated. This correlation was strongest in eastern and western parts of the USA and weak in northern states.

Our major finding of this study is over the course of the time series, at a monthly scale, the UVI has increased while total ozone has decreased in the continental US over the past three decades at four selected USDA stations while spatial distributions of UVI and total ozone have shown substantial variations from coastal zones to the Midwest Regions of the US. Yet the tendency toward recovery of ozone layer in the continental US can not be fully confirmed. This leads to a conclusion that the UVI changes might have been influenced by other factors in addition to the total ozone in the atmospheric environment across at least 76% of the continental USA. Yet very few studies are available to characterize temporal and regional variations in cloud cover, ozone column amount, boundary-layer ozone concentrations, and UV radiation as a whole. Future work may be directed toward exploring the global dimming impact and prove that atmospheric aerosols, cloud distribution, and other particulates have been linked to reductions in shortwave radiation and UVB measurements.

#### Acknowledgements

The authors of this paper are grateful for the financial support or technical support provided by Creative group project of national key lab (1088RA400SA), National 973 Key Project (2006CB403404) in China and "The Modification of Meteorological Observation of Anhui Province based on Technology of Remote Sensing and Modeling", USDA CSREES (2006-34263-16926) in the USA.

## References

1. Kerr, J.B.; Fioletov, V.E. Surface ultraviolet radiation. *Atmos-Ocean*. **2008**, *46*, 159–184.
2. Fioletov, V.E.; Bodeker, G.E.; Miller, A.J.; McPeters, R.D.; Stolarski, R. Global and zonal total ozone variations estimated from ground-based and satellite measurements: 1964–2000. *J. Geophys. Res. Atmos.* **2002**, *107*, 28032–29045.
3. Allen, D.R.; Reck, R.A. Daily variations in TOMS total ozone data. *J. Geophys. Res. Atmos.* **1997**, *102*, 13603–13608.
4. Bodeker, G.E.; Scott, J.C.; Kreher, K.; McKenzie, R.L. Global ozone trends in potential vorticity coordinates using TOMS and GOME intercompared against the Dobson network: 1978–1998. *J. Geophys. Res. Atmos.* **2001**, *106*, 23029–23042.
5. Reinsel, G.C. Seasonal trend analysis of published ground-based and TOMS total ozone data through 1991. *J. Geophys. Res. Atmos.* **1994**, *99*, 5449–5464.
6. Lapeta, B.; Engelsen, O.; Litynska, Z.; Kylling, B. Sensitivity of surface UV radiation and ozone column retrieval to ozone and temperature profiles. *J. Geophys. Res. Atmos.* **2000**, *105*, 5001–5007.
7. Gao, W.; Slusser, J.; Gibson, J.; Scott, G.; Bigelow, D.; Kerr, J.; McArthur, B. Direct-Sun column ozone retrieval by the ultraviolet multifilter rotating shadow-band radiometer and comparison with those from Brewer and Dobson spectrophotometers. *App. Opt.* **2001**, *40*, 3149–3155.
8. Herman, J.R.; Piacentini, R.D.; Ziemke, J.; Celarier, E.; Larko, D. Interannual variability of ozone and UV-B ultraviolet exposure. *J. Geophys. Res. Atmos.* **2000**, *105*, 29189–29193.
9. Krzyscin, J.W. Total ozone influence on the surface UV-B radiation in the late spring-summer 1963–1997: An analysis of multiple timescales. *J. Geophys. Res. Atmos.* **2000**, *105*, 4993–5000.
10. Malanca, F.E.; Canziani, P.O.; Arguello, G.A. Trends evolution of ozone between 1980 and 2000 at midlatitudes over the Southern Hemisphere: Decadal differences in trends. *J. Geophys. Res. Atmos.* **2005**, *110*, 30601–30611.
11. Rusch, D.W.; Clancy, R.T.; Bhartia, B.K. Comparison of satellite measurements of ozone and ozone trends. *J. Geophys. Res. Atmos.* **1994**, *99*, 20501–20511.
12. McCormack, J.P.; Hood, L.L. Modeling the spatial distribution of total ozone in northern hemisphere winter: 1979–1991. *J. Geophys. Res. Atmos.* **1997**, *102*, 13711–13717.
13. McKenzie, R.; Conner, B.; Bodeker, G. Increased summertime UV radiation in New Zealand in response to ozone loss. *Science* **1999**, *285*, 1709–1711.
14. Miller, A.J. Comparisons of observed ozone trends and solar effects in the stratosphere through examination of ground-based Umkehr and combined solar backscattered ultraviolet (SBUV) and SBUV 2 satellite data. *J. Geophys. Res. Atmos.* **1996**, *101*, 9017–9021.
15. Tourpali, K.; Tie, X.X.; Zerefos, C.S.; Brasseur, G. Decadal evolution of total ozone decline: Observations and model results. *J. Geophys. Res. Atmos.* **1997**, *102*, 23955–23962.
16. Ziemke, J.R.; Herman, J.R.; Stanford, J.L.; Bhartia, P.K. Total ozone UVB monitoring and forecasting: Impact of clouds and the horizontal resolution of satellite retrievals. *J. Geophys. Res. Atmos.* **1998**, *103*, 3865–3871.
17. Chubarova, N.Y.; Nezval, Y.I. Thirty year variability of UV irradiance in Moscow. *J. Geophys. Res. Atmos.* **2000**, *105*, 12529–12539.

18. Eckman, R.S.; Grose, W.L.; Turner, R.E.; Blackshear, W.T. Polar ozone depletion: A three-dimensional chemical modeling study of its long-term global impact. *J. Geophys. Res. Atmos.* **1996**, *101*, 22977–22989.
19. WHO. *Global Solar UV Index: A practical guide*. World Health Organization (WHO), World Meteorological Organization (WMO), United Nations Environment Program (UNEP), and International Commission on Non-Ionising Radiation Protection (ICNRP): Geneva, Switzerland, 2002.
20. Komhyr, W.D. *Operations Handbook—Ozone Observations with a Dobson Spectrophotometer*; WMO Global Ozone Research and Monitoring Project Report 6. World Meteorological Organization: Geneva, Switzerland, 1980.
21. Dobson, G.M.B. Observers' handbook for the ozone spectrophotometer. In *Annals of the International Geophysical Year*, 5 (part I); Pergamon: New York, NY, USA, 1957; pp. 46–89.
22. McPeters, R.D.; Bhartia, P.K.; Krueger, A.J.; Herman, J.R. *Earth Probe Total Ozone Mapping Spectrometer (TOMS) Data Products User's Guide*. NASA Technical Publication, 1998–206895, Goddard Space Flight Center Greenbelt: Greenbelt, MD, USA, 1998.
23. McKinlay, A.F.; Diffey, B.L. A reference spectrum for ultraviolet induced erythema in human skin. In *Human Exposure to Ultraviolet Radiation: Risks and Regulations*; Passchler, W.R., Bosnjakovic, B.F.M., Eds.; Elsevier: Amsterdam, the Netherlands, 1987.
24. World Meteorological Organization. *Scientific Assessment of Ozone Depletion: 2006*. Available online: [http://www.wmo.int/pages/prog/arep/gaw/ozone\\_2006/ozone\\_asst\\_report.html](http://www.wmo.int/pages/prog/arep/gaw/ozone_2006/ozone_asst_report.html) (Accessed on 4 January 2010).
25. Hofmann, D.J.; Oltmans, S.J.; Harris, J.M.; Johnson, B.J.; Lathrop, J.A. Ten years of ozonesonde measurements at the south pole: implications for recovery of springtime Antarctic ozone. *J. Geophys. Res.* **1997**, *102*, 8931–8943.
26. Andersen, S.B.; Weatherhead, E.C.; Stevermer, A.; Austin, J.; Fleming, E.L. Comparison of recent modeled and observed trends in total column ozone. *J. Geophys. Res.* **2006**, *111*, 1–10.
27. Elizabeth, C.W.; Signe, B.A. The search for signs of recovery of the ozone layer. *Nature* **2006**, *441*, 39–45.
28. Reinsel, G.C.; Miller, A.J.; Elizabeth, C.W.; Lawrence, E.F. Trend analysis of total ozone data for turnaround and dynamical contributions. *J. Geophys. Res.* **2005**, *110*, D16306.
29. Reinsel, G.C.; Elizabeth, C.W.; George, C.T.; Alvin, J.M. On detection of turnaround and recovery in trend for ozone. *J. Geophys. Res.* **2002**, *107*, D104078.
30. Newchurch, M.J.; Yang, E.S.; Cunnold, D.M.; Reinsel, G.C. Evidence for slowdown in stratospheric ozone loss: First stage of ozone recovery. *J. Geophys. Res.* **2003**, *108*, D164507.
31. Hadjinicolaou, P.; Pyle, J.A.; Harris, N.R.P. The recent turnaround in stratospheric ozone over northern middle latitudes: A dynamical modeling perspective. *Geophys. Res. Lett.* **2005**, *32*, L12821.
32. Schnadt, C.; Dameris, M.; Ponater, M.; Hein, R.; Grewe, V.; Steil, B. Interaction of atmospheric chemistry and climate and its impact on stratospheric ozone. *Clim. Dyn.* **2002**, *18*, 501–517.